

# Quantifying metallurgical interactions in solid/liquid diffusion couples using differential scanning calorimetry

M.L. Kuntz \*, S.F. Corbin, Y. Zhou

*Department of Mechanical Engineering, University of Waterloo, 200 University Ave. W., Waterloo, Canada ON N2L 3G1*

Received 14 December 2004; received in revised form 11 March 2005; accepted 16 March 2005

Available online 14 April 2005

## Abstract

A novel method using differential scanning calorimetry (DSC) has been developed to quantify the interface kinetics in a solid/liquid diffusion couple. The Ag–Cu binary eutectic system is investigated by heating an assembly of Ag base metal and Ag–Cu eutectic foil to 800 °C and holding. The fraction of liquid remaining after various isothermal hold periods is measured by comparing the melting endotherms with the solidification exotherms. Detailed analysis of the results show the per cent liquid remaining is inversely proportional to the square root of isothermal hold time; however, effects of the base metal cause an apparent loss of 25% of the liquid immediately after heating. The fundamental understanding of the effects of bi-phase diffusion couple geometry is advanced to manifest the mechanisms resulting in the error. Further carefully devised experiments reveal that primary solidification during cooling is not included in the enthalpy of solidification measured by the DSC. Furthermore, baseline shift across the melting endotherm increases the measured melting enthalpy. These effects combine to systematically underestimate the fraction of liquid remaining. Development of a modified temperature program and application of an appropriate correction can remedy these effects. The experimental results compare well with a prediction generated by an analytical model. Successful quantification of these phenomena has broadened the knowledge of DSC operational characteristics in the solid/liquid diffusion couple treatment, which can now be applied to other material systems.

© 2005 Acta Materialia Inc. Published by Elsevier Ltd. All rights reserved.

*Keywords:* Differential scanning calorimetry; Isothermal solidification; Diffusion; Interface dynamics; Kinetics

## 1. Introduction

Metallurgical interactions that take place between a liquid and solid phase in metal alloys are fundamental in many materials processing operations. These include: soldering and brazing, where a molten filler metal wets a solid metal substrate [1]; homogenization of castings via partial melting [2]; metallurgical coating operations such as aluminizing or galvanizing, where a solid alloy part is dipped in a molten metal bath [3]; composite fabrication by infiltration techniques, where a liquid metal matrix penetrates a solid skeleton network under pressure or

by capillary action [4]; and liquid phase sintering of powder compacts [5,6]. In all these cases the solid and liquid phases are metallurgically dissimilar and a diffusion couple develops at the solid/liquid interface. The metallurgical interactions at this interface can be dissolution of soluble elements and/or the formation of homogeneous or intermediate phases. In either case, the phases that form are critical to the processing operation. For example, in soldering and brazing these metallurgical interactions determine the strength of the joint formed between dissimilar materials and the reliability of components assembled from them [1]. In metallurgical coating operations these interactions determine not only the adhesion of the coating but also the wear or corrosion resistance of the coated part [7]. Thus, it is

\* Corresponding author. Tel.: +1 519 888 4567.

E-mail address: [mlkuntz@uwaterloo.ca](mailto:mlkuntz@uwaterloo.ca) (M.L. Kuntz).

desirable to have an accurate measure of the reaction kinetics.

The investigation of phase formations occurring in a solid/liquid diffusion couple have traditionally been completed by performing the coating and/or joining operation followed by cooling or quenching and metallurgical examination of the phases formed at the interface. Metallographic techniques have been subject to a great deal of measurement error since the solid/liquid interface is usually not planar but scalloped. Thus, manual measurements of the width of the solidified layer are largely subjective. Furthermore, only a small portion of the solid/liquid interfacial area is often measured. MacDonald and Eagar [8] have shown that experimental set-up can also be a source of significant error. The apparent overall reaction kinetics can be increased by the loss of liquid from a joint interface, either by squeezing or through wetting of the sides of the base metal. Therefore, a method of characterizing the process kinetics of a solid/liquid diffusion couple that is not subject to these experimental errors is required.

Previous work has been successful in applying differential scanning calorimetry (DSC) to the quantification of solid/liquid phase interactions in a powder mixture analogous to transient liquid phase sintering (TLPS) [9]. The amount of eutectic liquid remaining in a TLPS mixture at the eutectic temperature,  $T_E$ , was quantified. This was done by cooling the samples from  $T_E$  after various hold times and measuring the enthalpy of the eutectic solidification peak. The reduction in the magnitude of the enthalpy of solidification was then related to the amount of liquid remaining.

The primary difference between solid/liquid diffusion couples developed in a powder mixture and that on a planar front relates to the geometry of the two problems. It is anticipated that these geometrical differences will have a large impact on the way in which DSC must be used to quantify the metallurgical reactions taking place at a planar interface. In powder mixtures the liquid phase is present in relatively high weight fractions (5–50 wt.%) and the liquid comes into contact with a high solid surface area during processing. In a planar geometry the liquid is present in a much smaller weight fraction (i.e., <0.1 wt.%) and should only come in contact with the faying surface of the solid for correct interpretation of the problem. The large mass of solid substrate in a planar type geometry may alter the heat flow characteristics in the DSC, which need to be accounted for.

Therefore, the primary objectives of this investigation are: to develop a methodology using DSC that would be capable of quantifying the metallurgical reactions taking place between solid/liquid diffusion couples, and to explain the effects of a planar geometry on the measured results.

## 2. Experimental set-up

The problem of interest is a bi-phase diffusion couple involving a solid base metal and liquid phase separated by a definite interface. Furthermore, we consider the case where the liquid phase is present as a thin film on a semi-infinite solid substrate. This diffusion couple yields a typical moving boundary problem as described in Fig. 1. For the purposes of a solid/liquid diffusion couple, the simplifying assumptions made in the construction of Fig. 1 include: local equilibrium at the solid/liquid interface; a semi-infinite solid phase; and no concentration gradient in the liquid phase. The latter assumption has been shown in the literature to be reasonable [10].

A more complicated binary alloy problem can also be envisioned where a series of intermediate phases could form between the liquid phase and solid base metal. Similarly, over time these intermediate phases will grow with diffusion into the base metal, leading to a reduction in the liquid present. Yet another similar problem could be defined where the diffusion couple involves a ternary (or multi-component) composition. In this case diffusion into the base metal by two solute atoms can lead to a shifting liquid composition as well as a reduction in the liquid phase [11]. However, the scope of the current investigation is that of a simple bi-phase binary diffusion couple.

In order to develop a DSC methodology capable of studying the various solid/liquid diffusion couple problems described above, a simple Ag–Cu binary eutectic was selected for an ideal model system. Pure Ag was selected for the solid phase (base metal) and a Ag–Cu alloy for the liquid phase. The binary equilibrium phase diagram shows the system is a simple binary with a eutectic at 780 °C and 28 wt.% Cu, and that no stable

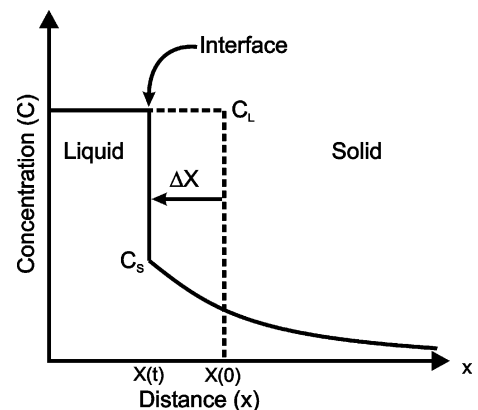


Fig. 1. A diffusion couple and moving boundary problem in a simple solid/liquid system. After a time step,  $\Delta T$ , the interface has moved  $\Delta X$ . The solid and liquid concentrations,  $C_S$  and  $C_L$ , respectively, are expected to obey the phase boundaries on the equilibrium phase diagram shown in Fig. 2.

intermetallics will form [12]. Furthermore, Ag can be considered inert up to the process temperature; thus, the formation of contaminants (e.g., oxides) which could inhibit isothermal solidification is not expected to be significant on the surface of the solid.

Right cylinders with a diameter of 5 and 3 mm thickness were prepared using 99.95% pure Ag obtained from Alfa Aesar. The faying surface was ground flat with 1200 grit paper and cleaned ultrasonically with acetone before processing. The liquid phase was added in the form of a thin foil with a Ag–Cu eutectic composition: Ag–28 wt.% Cu. The foil was obtained from Lucas Milhaupt and had a purity of 99.9%. The interlayer thickness was 25  $\mu\text{m}$  and it was cleaned ultrasonically with acetone before joining. In order to interpret dissolution effects and the resultant shift in liquid compositions, a 24-wt.% Cu foil corresponding to the liquidus composition at the hold temperature was also studied. This foil was not commercially available and was fabricated by casting from high purity powders. The cast ingot was then rolled to a thin foil in a series of steps, each step followed by a recovery anneal.

The side of the cylinder was coated with an alumina lubricant to prevent the liquid from wetting any surface of the cylinder other than the faying surface. A diffusion couple was placed in an alumina crucible for heating in the DSC as shown in Fig. 3. The foil that will melt upon heating through the eutectic temperature is placed at the bottom of the crucible so that the liquid zone will be as close as possible to the measuring thermocouples in the DSC. This ensures maximum sensitivity of the measurement system. In the reference crucible, a plain Ag slug was added to ensure that the thermal properties of both cells were similar. Thus, the only difference between the sample and reference cells is the presence of the melting point depressant rich foil.

Interface movement is expected to obey the mass balance given by Eq. (1):

$$(C_L - C_S) \frac{d}{dt} X(t) = D_S \frac{\partial}{\partial x} C_S - D_L \frac{\partial}{\partial x} C_L, \quad (1)$$

where  $C_L$  and  $C_S$  are the respective liquid and solid concentrations at the solid/liquid interface,  $X(t)$  is the position of the interface, and  $D_S$  and  $D_L$  are the solute diffusivities in the solid and liquid, respectively.

Upon heating above the eutectic temperature, the foil will melt and wet the substrate. Additional heating above the eutectic will cause the interface in Fig. 1 to move to the right as the liquid tracks along the Gibbs phase boundaries on the equilibrium diagram schematic for a binary eutectic shown in Fig. 2. This dissolution of the base metal results in widening of the liquid layer until the maximum liquid width is reached at the peak temperature. If the temperature is held, the solidus and liquidus concentrations at the interface will be constant as predicted by the tie line in Fig. 2. Inspection of Eq. (1)

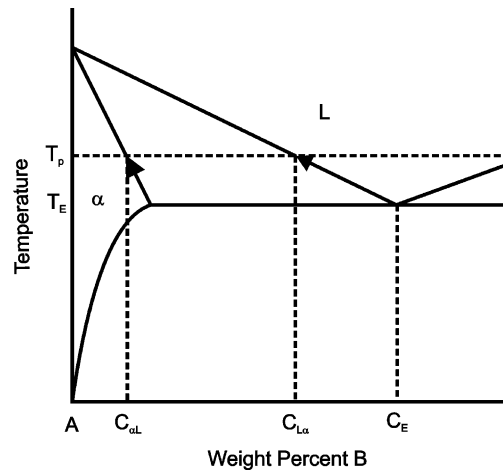


Fig. 2. Equilibrium phase diagram for a simple binary eutectic system. The solidus ( $C_S$ ) and liquidus ( $C_L$ ) concentrations at the interface are given by the phase boundaries ( $C_{sL}$  and  $C_{Ls}$ ) at the process temperature.

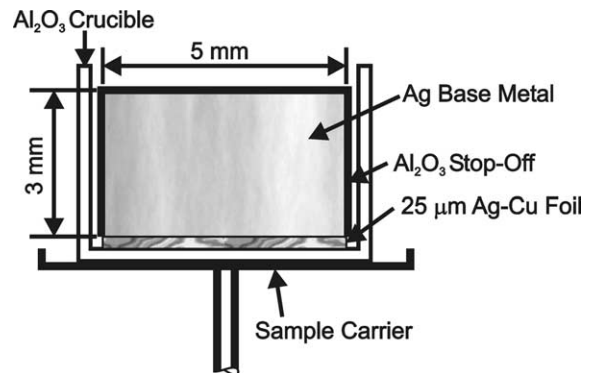


Fig. 3. A typical cross-section of the experimental set-up within the DSC sample carrier. The Ag cylinder is coated with a ceramic stop-off and placed on a disc of foil.

indicates that diffusion of solute from the liquid into the solid phase results in solid/liquid boundary movement to the left in Fig. 1 and a resulting reduction in the amount of liquid phase. This mechanism of epitaxial growth of the solid is commonly termed isothermal solidification [13].

A Netzsch 404C differential scanning calorimeter was used for the experiments. A dynamic nitrogen atmosphere was used in the DSC for all trials. A typical thermal cycle of a DSC trial is given in Fig. 4. The initial heating rate was 40  $^{\circ}\text{C}/\text{min}$  (segment A). At 700  $^{\circ}\text{C}$ , the heating rate was reduced to 10  $^{\circ}\text{C}/\text{min}$  for enhanced measurement resolution and reduced thermal lag in the temperature range of interest (segment B). The hold temperature was 20  $^{\circ}\text{C}$  above the eutectic temperature of 780  $^{\circ}\text{C}$  (i.e., 800  $^{\circ}\text{C}$ ). This superheating was the minimum needed to completely resolve the melting peak of the initial liquid on the DSC trace. The isothermal hold time at the bonding temperature was varied from zero to

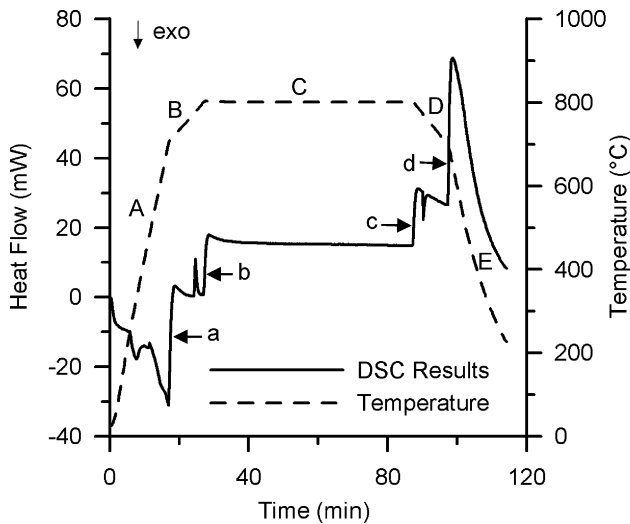


Fig. 4. The temperature program for a typical DSC trial and the corresponding DSC trace. The isothermal hold time (segment C) is varied.

the time required for isothermal solidification to near completion (segment C). The cooling cycle was opposite the heating cycle (segments D and E).

### 2.1. Analysis method

The DSC heat flow results that correspond to the sample temperature program are shown by the solid line in Fig. 4. On the DSC trace the exothermic direction is down, thus a peak represents an endothermic phase change such as melting, and a trough represents an exothermic phase change such as solidification. The segments of the heat flow curve marked a–d are baseline shifts (hysteresis) due to alterations in the heating rate. Eq. (2) gives the temperature difference ( $\Delta T$ ) between the reference cell ( $T_{rm}$ ) and the sample cell ( $T_{sm}$ ),

$$\Delta T = T_{rm} - T_{sm} = R \frac{dT}{dt} (C_s - C_r), \quad (2)$$

where  $R$  is the thermal resistance, and  $C_s$  and  $C_r$  are the heat capacities of the sample and reference cells, respectively [14].

A change in the heating rate ( $dT/dt$ ) results in a shift in  $\Delta T$  corresponding to the observed hysteresis shifts in the DSC trace. The heating and cooling segments at 10 °C/min (B and D), which pass through the melting temperature of the Ag–Cu eutectic foil (i.e., 780 °C) are the segments used to quantify isothermal solidification.

Athermal segments of the DSC trace can also be plotted as a function of heat flow versus temperature (see Fig. 5). Integration of the melting endotherm (heating segment peak, i.e., 448 mJ) or solidification exotherm (cooling segment peak, i.e., 126 mJ) gives the total enthalpy of the thermal event. Since the composition of the liquid is constant throughout the isothermal solidifi-

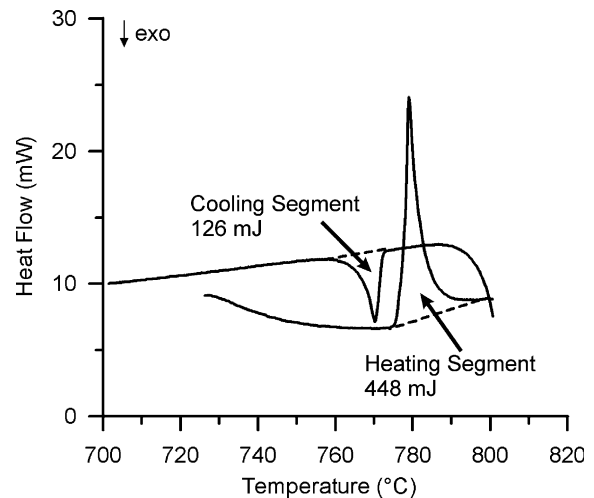


Fig. 5. The DSC results plotted as a function of temperature. The integral of the exotherm (cooling segment) and endotherm (heating segment) is shown.

cation stage, the specific heat of formation of the liquid,  $\Delta h_f$  will remain unchanged. Note that the peak temperature used in these experiments must be sufficiently higher than the solidus temperature so that the DSC trace returns to baseline allowing the area under the endotherm to be measured.

A baseline value for the enthalpy of formation ( $\Delta h_f$ ) as measured for the Ag–Cu eutectic foil alone was 116 and 114 mJ/g for melting and solidification, respectively, for a foil with a mass of 5.3 mg. The small difference between these measurements is attributed to variation in the measurement system and is expected.  $\Delta H_s$  is the enthalpy measured from the solidification exotherm in a DSC diffusion couple experiment. Since the mass of liquid involved in solidification is given by  $\Delta H_s / \Delta h_f$ ; where  $\Delta h_f$  is constant, the enthalpy of formation can be used as a reference to determine the amount of liquid remaining (and thus interface position) in a solid/liquid diffusion couple after an isothermal hold period. Eq. (3) gives this relationship:

$$\% \text{ Liquid remaining} = 100 \times \frac{\Delta H_s}{\Delta h_f m}, \quad (3)$$

where  $m$  is the mass of the original eutectic foil.

### 2.2. Influence of base metal on measurements

The ratio of foil mass to base metal mass is less than one per cent and, since the large solid mass is not involved in the phase change, the influence on thermal characteristics should be determined. Therefore, an experimental method was devised to determine the melting endotherm in the presence of the base metal, but in the absence of metallurgical interaction. In this case, an  $\text{Al}_2\text{O}_3$  diffusion barrier was applied to the base metal surface in contact with the eutectic foil to prevent metal-

Table 1  
DSC measurements of enthalpy of formation of Ag–Cu foil with and without the presence of base metal

DSC type	Average melting onset (°C)	Average initial enthalpy (mJ/g)	Average final enthalpy (mJ/g)
Foil only	775	116	114
Foil with base metal	776	85	85

An Al<sub>2</sub>O<sub>3</sub> diffusion barrier was used to prevent interaction between the liquid and base metal.

lurgical interactions and the  $\Delta H_f$  measured. The results are shown in Table 1. Clearly, the base metal acts as a heat sink in the measurement cell and, by conduction, reduces the total heat of formation measured by the DSC from 115 to 85 mJ/g.

The mass of the base metal varies slightly from sample to sample, so the heat sink effects are expected to vary as well. Thus, it is considered more accurate to determine the percentage of liquid remaining by taking a ratio of the solidification exotherm ( $\Delta H_s$ ) to the initial melting endotherm ( $\Delta H_m$ ) as measured in each DSC trial, given by Eq. (4) in this manner, the heat flow influence from the base metal is constant during melting and solidification,

$$\% \text{ Liquid remaining} = 100 \times \frac{\Delta H_s}{\Delta H_m}. \quad (4)$$

### 3. Preliminary results and problem

The enthalpy measurements of the bi-phase diffusion couple experiments are given in Table 2 with the per cent liquid remaining calculated using Eq. (4) [15]. As expected, the amount of liquid remaining decreases with

increased isothermal hold time as the solid/liquid interface advances into the liquid phase. The per cent liquid remaining is inversely proportional to the square root of isothermal hold time as shown in Fig. 6. The coefficient of determination ( $R^2$ ) for the linear regression fit applied to the data in Fig. 6 is 0.992. This infers good precision of the measurement system. By extrapolating the trend line forward to zero per cent liquid remaining, the time required for the completion of isothermal solidification can be found (i.e., 15.5 h). Conversely, the trend line can be extrapolated back to the start of the isothermal hold period. Examination of Fig. 6 reveals that the trend line does not intersect the liquid remaining axis at unity, but instead at 75%. This result is counter-intuitive; furthermore, it makes a comparative measure of the interface kinetics impossible.

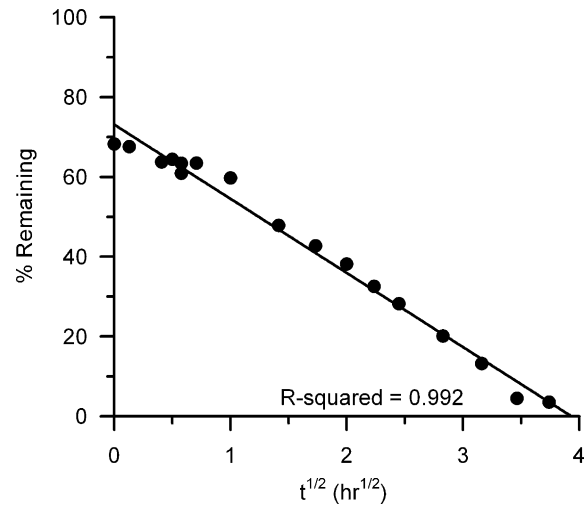


Fig. 6. Per cent liquid remaining as a function of the square root of isothermal hold time.

Table 2  
Results of DSC experiments with a eutectic Ag–Cu foil

Isothermal hold time (h)	Square root time (h <sup>1/2</sup> )	Foil mass (mg)	Melting onset (°C)	Initial enthalpy (mJ), $\Delta H_m$	Final enthalpy (mJ), $\Delta H_s$	% Liquid remaining
0	0.00	5.30	777	514	351	68.23
0.017	0.13	5.20	777	499	337	67.58
0.17	0.41	5.20	777	460	293	63.73
0.25	0.50	5.10	777	418	269	64.44
0.33	0.58	5.10	777	468	297	63.42
0.33	0.58	5.30	778	495	302	60.91
0.5	0.71	5.14	777	385	244	63.49
1	1.00	5.20	776	341	204	59.77
2	1.41	5.19	777	408	195	47.88
3	1.73	5.20	777	449	192	42.72
4	2.00	5.19	777	482	184	38.20
5	2.24	5.21	777	460	150	32.62
6	2.45	5.27	777	448	126	28.22
8	2.83	5.11	777	407	82	20.13
10	3.16	5.25	778	510	68	13.25
12	3.46	5.17	777	445	20	4.51
14	3.74	5.18	776	440	16	3.56

The loss of 25% of the initial liquid formed during very short isothermal hold times may be due to transient effects at the beginning of isothermal solidification. Due to the nature of the DSC experiments (i.e. required heating and cooling rates), the actual time above the eutectic temperature is over 3 min when the nominal isothermal hold time is zero. Thus, measurement data to verify the non-linearity of the results could not be collected. A review of relevant literature did not provide a physical explanation for this; therefore, the apparent loss of liquid is more likely an artifact of the experiment.

The DSC data generated by the diffusion couple experiments can be exploited to provide a physical understanding of the aberration in the results.

## 4. Results and discussion

### 4.1. Influence of eutectic foil thickness

The DSC diffusion couple experiments were repeated with thicker liquid widths and no isothermal hold time. The results given in Table 3 show that roughly the same fraction of liquid remains regardless of the initial liquid width. The increase in the fraction of liquid remaining from 5.30 mg (initial eutectic foil mass) to 10.3 mg is likely due to time dependant dissolution of the base metal. With the thicker foil, there is more dissolution during heating. Hence, with thicker foils, the dissolution may not be instantaneous as it is assumed with the thin foil, resulting in less liquid measured upon melting. Also, any interface movement that occurs during the 3-min above the eutectic represents a larger fraction of the thinnest foil, which agrees with the measurements. If there was a transient effect at the beginning of the isothermal solidification process, the absolute width of liquid consumed would be independent of the initial liquid width. This elucidates the argument that the apparent liquid loss is due to the measurement system and not physical interaction between the phases.

### 4.2. Influence of primary solidification

During the TLP bonding of Ni using a Ni–P interlayer, Saida et al. [16] found that the fraction of the li-

quid solidified as primary Ni was affected by the cooling rate. Campbell and Boettinger [17] later confirmed this in the Ni–Al–B system. In the DSC experiments the cooling rate is 10 °C/min during cooling from the process temperature (800 °C) to the eutectic temperature (780 °C). Thus it is expected that some primary  $\alpha$ -phase solidification will occur.

Metallurgical examination of the interface of a DSC diffusion couple after cooling from an isothermal hold period shows a fine lamellar eutectic structure. The base metal adjacent to the interface shown in Fig. 7 has undergone a solid-state transformation upon cooling below the solvus temperature following solidification. This cellular precipitation in the Cu-saturated base metal has obscured the underlying solidification structure [18,19]. The scalloped interface; however, provides some evidence that epitaxial solidification has occurred in a cellular mode. Thus, it is likely that athermal primary solidification has occurred at the solid/liquid interface.

Upon cooling from the isothermal hold temperature, heterogeneous nucleation of  $\alpha$ -phase occurs almost immediately at the solid/liquid interface. The primary phase then grows into the liquid, rejecting solute as the temperature decreases. This would lead to an expected exothermic peak on the DSC trace; however, it is conspicuously absent in all results. Conversely, after the required undercooling below  $T_E$ , eutectic solidification is initiated. This releases a sharp burst of energy, resulting in a very well defined exothermic peak with a clear onset temperature that is separated from the primary solidification event (e.g., well illustrated in the cooling trace of Fig. 6). Therefore, it appears the measured exothermic energy ('final enthalpy,  $\Delta H_s$ ' in Table 2) includes only the eutectic fraction of the solidified liquid.

Fig. 8 provides an explanation of diffusion couple melting and solidification along with the corresponding DSC trace segment. During heating the endothermic peak on the DSC trace begins at the onset of eutectic foil melting. In the absence of any thermal lag, the melting endotherm of a eutectic phase should appear as a single,

Table 3  
Results of multi-thickness DSC study

Foil mass (mg)	Melting onset (°C)	Initial enthalpy (mJ), $\Delta H_m$	Final enthalpy (mJ), $\Delta H_s$	% Liquid remaining
5.30	777	514.3	350.9	68.2
10.3	778	884.3	702.4	79.4
14.8	779	1411	1085	76.9
20.7	778	1806	1423	78.8
25.9	779	2317	1844	79.6

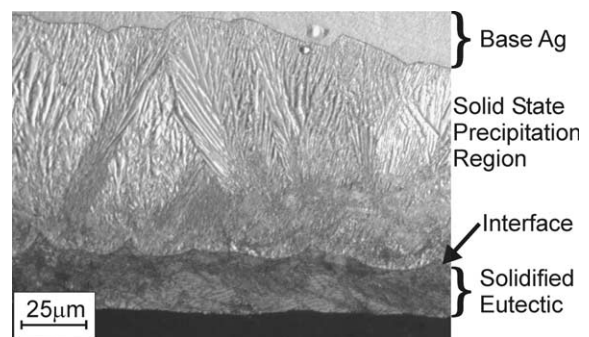


Fig. 7. Optical micrograph of the interface showing the solidified eutectic and the cellular precipitation adjacent to the interface.

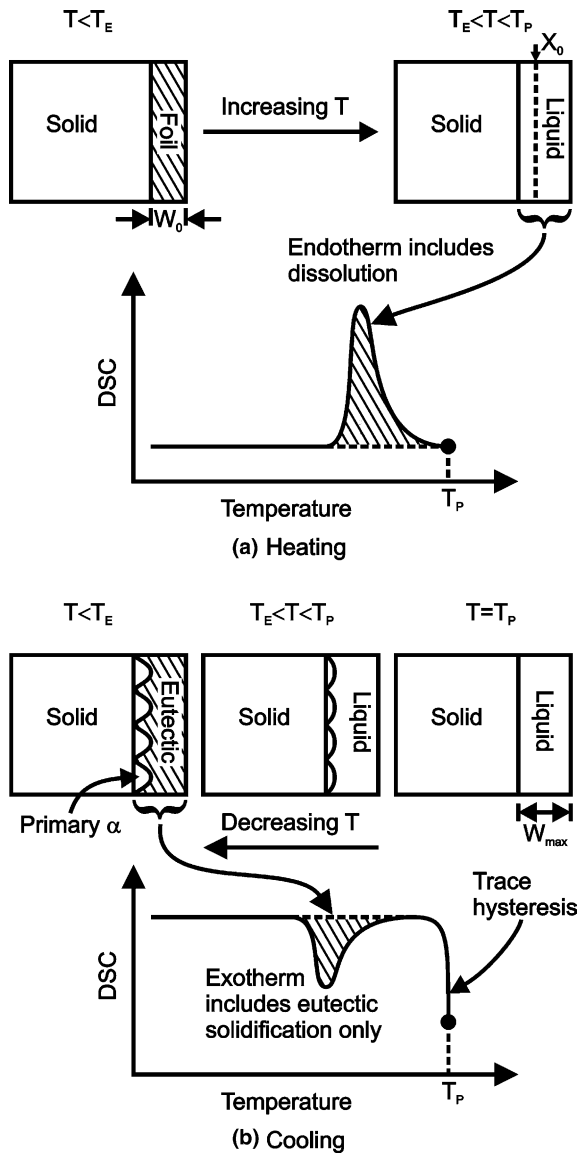


Fig. 8. Schematic of phase change and corresponding DSC trace segment: (a) heating above  $T_E$ , and (b) cooling from  $T_P$  through  $T_E$ .

narrow and sharp peak. However, the presence of the Ag base metal will tend to increase thermal lag and the endotherm appears as a broadened peak. During this elapsed time the eutectic liquid wets with the faying surface of the base metal and, as the sample is heated from  $T_E$  to  $T_P$ , dissolution of the base metal Ag will increase the liquid formed. As a result it is argued that at least part of the energy of dissolution is included in the measured endothermic energy ('initial enthalpy,  $\Delta H_m$ ' in Table 2).

The calculation of 'per cent liquid remaining' in Table 2 requires calculation of  $\Delta H_s/\Delta H_m$ , and since the exothermic energy includes only the eutectic fraction of solidified liquid, Eq. (4) will report lower than actual values. To confirm the effect of the primary solidification phenomenon further, a hypoeutectic foil with a compo-

sition of 24% Cu (liquidus at 800 °C) was prepared and subjected to the same DSC heating cycle. Similar to the experiments of Table 1, an  $Al_2O_3$  barrier was placed between the foil and Ag base metal to prevent metallurgical interaction; the resulting DSC trace is given in Fig. 9. Fig. 10 illustrates a parallel experiment where the foil was of the normal eutectic composition. The first observation from Fig. 9 is that the cooling segment shows two exothermic peaks. The first peak is due to the primary  $\alpha$ -phase solidification, while the second (larger) peak represents the enthalpy of the eutectic solidification. The solidified microstructure, shown in Fig. 11, differs from the solidification structure of the diffusion couple (Fig. 7), both starting with the same liquid composition.

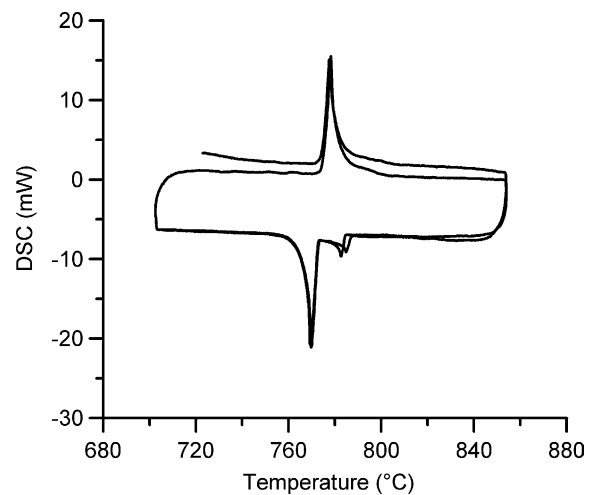


Fig. 9. DSC trace of Ag-24% Cu foil with a diffusion barrier between liquid and base metal to prevent metallurgical interaction. Two heating and cooling cycles are shown.

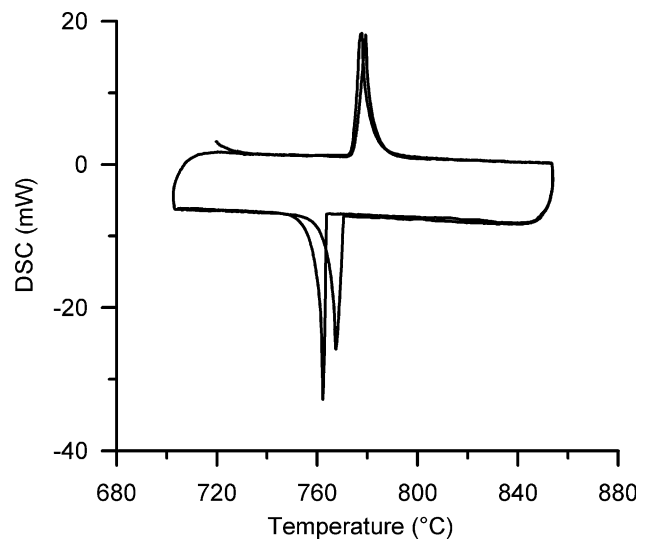


Fig. 10. DSC trace of eutectic foil with a diffusion barrier between liquid and base metal to prevent metallurgical interaction. Two heating and cooling cycles are shown.

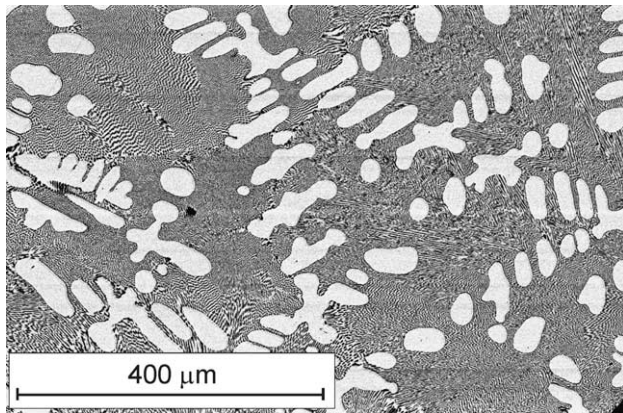


Fig. 11. Solidified microstructure of Ag–24% Cu cooled at 10 °C/min.

The primary  $\alpha$ -phase (white) is clearly shown in the eutectic matrix; the solidification structure is distinguished by the dendritic nature and is indicative of a solidification process requiring nucleation. This is consistent with the fact that the measured onset temperature of the primary phase solidification exotherm in Fig. 9 was 786 °C (i.e., 14 °C undercooling). This provides further evidence that primary solidification is occurring in the diffusion couple of Fig. 5 but in an epitaxial manner such that the exothermic energy associated with it is not visible on the DSC trace. It is also worth noting that the second solidification peak in Fig. 9 has a very similar shape (i.e., a sharp onset) and onset temperature as the eutectic foil of Fig. 10. Both these peaks are also very similar in shape and onset temperature as the solidification peak from the diffusion couple of Fig. 5. This confirms that the solidification peaks that are observed in the diffusion couple experiments of Fig. 6 and measured in Table 2 (i.e., final enthalpy) are due only to the solidification of the eutectic.

The second observation is that the shape of the melting endotherm for the off-eutectic foil does not indicate separate melting peaks for the eutectic and primary phase that it contains. (i.e., these melting events overlap). This shows that in the case of the eutectic/Ag diffusion couple, if melting due to dissolution of the base metal was taking place during heating it would not show as a separate peak in a trace such as Fig. 6. Therefore, it can be concluded that the endothermic energy measured from the initial melting peak may include dissolution of the base metal.

The above arguments indicate that the measured solidification exothermic energy,  $\Delta H_s$ , includes only the solidification of the eutectic fraction remaining in the sample and not the entire liquid. Conversely the melting endothermic energy,  $\Delta H_m$ , may contain not only the initial eutectic but also some dissolution. Therefore, calculating the per cent liquid remaining by Eq. (4) yields a systematic underestimation of the liquid fraction present after an isothermal hold time.

From the DSC trace of Fig. 9 the exothermic energy from the solidification of eutectic phase can be determined (i.e., 73 J/g), and compared to the value obtained from the parallel trace for eutectic foils only from Fig. 10 (i.e., 101 J/g). This reveals that, for the hypoeutectic liquid, the endothermic energy of the eutectic portion is approximately 72% of the total endothermic energy due to solidification of the liquid remaining (note; however, that the primary and eutectic exotherms overlap in Fig. 9, which will decrease the measured enthalpy, possibly as much as 10%). This agrees with the measurement of area fraction of  $\alpha$ -phase Ag in the microstructure of Fig. 11, measured using image analysis software to be 25%. Therefore, it can be suggested that the exothermic energies for the final enthalpy in Table 2 represents only 75% of the total liquid remaining in the sample after a specific hold time, and that the apparent loss of 25% of the liquid at zero hold time in Fig. 5 is the fraction of primary solidification.

Interestingly, the problem of liquid loss at short hold times has been found in the literature, but not explored. Venkatraman et al. [20] noticed that the fraction of liquid remaining did not extrapolate to unity in their study of isothermal solidification in electroplated Au–Sn layers on Cu. The investigators offered that the lack of experimental data at short hold times along with a decrease in the isothermal solidification rate due to solute saturation was responsible; however, it is possible that the primary solidification of a fraction of liquid was missed. If the data were adjusted to account for the primary solidification, the experimental results would likely agree more closely with the modeled results [21].

#### 4.3. Influence of interface development and baseline shift

It is now quite certain that epitaxial primary solidification during cooling from temperatures above the eutectic is not measured by the DSC, and a correction factor to take this into account results in the desired effect. However, the concept of this correction relies on the assumption that the initial melting endotherm measures the complete dissolution process expected when the eutectic liquid is in perfect contact with the faying surface of the Ag base.

Inspection of the melting endotherm reveals some interesting trends. The melting endotherm of the hypoeutectic 24% Cu foil (Fig. 9) shows a tail which is indicative of additional, prolonged melting and consistent with what would be expected with dissolution of the primary phase. Comparison with the endotherm from a typical diffusion couple does not yield a similar result. Therefore, there is some question as to the extent of dissolution taking place during initial heating, and the fraction of which is included in the melting endotherm. The corollary is that the effect of primary solidification alone does not completely explain discrepancies in Fig. 5. This

can be further explored by an investigation of the baseline shift in the DSC trace.

A shift in the baseline across a peak of a phase transformation under constant heating is an indication of a change in the specific heat of the sample, which is expected to occur with a change of phase (i.e., in the current case, the melting of the eutectic foil). The magnitude of the observed shift (Fig. 12) is greater than what is expected for the melting of the foil. Furthermore, the dramatic baseline shift in Fig. 12 occurs only on the initial heating segment and not on the cooling segment. There is also no dramatic shift on subsequent heating segments when a re-melt schedule is used. Thus, the baseline shift observed on the first cycle is not attributed to a change in the specific heat of the melting foil only.

It is argued that in this work, the cause of the shift in the DSC trace baseline is due to changes in the thermal coupling of the crucible and the sample before and after melting. This can be described with reference to Fig. 13. Before melting, there are two interfaces between the Ag base metal and the crucible: the crucible/foil interface and the foil/base metal interface. During initial heating, these interfaces are unbonded, mechanical interfaces with a certain thermal contact resistance. Upon melting, the foil wets and bonds to the base metal and, while there are still two interfaces between the base metal and the crucible, the thermal coupling of the metallurgical solid/liquid interface is much better for heat conduction. The thermal resistances across these interfaces are part of the thermal characteristics of the DSC cell and as shown by Eq. (2), a change in the thermal resistance,  $R$ , will result in a DSC trace baseline shift that is unrelated to the hysteresis discussed in Fig. 4.

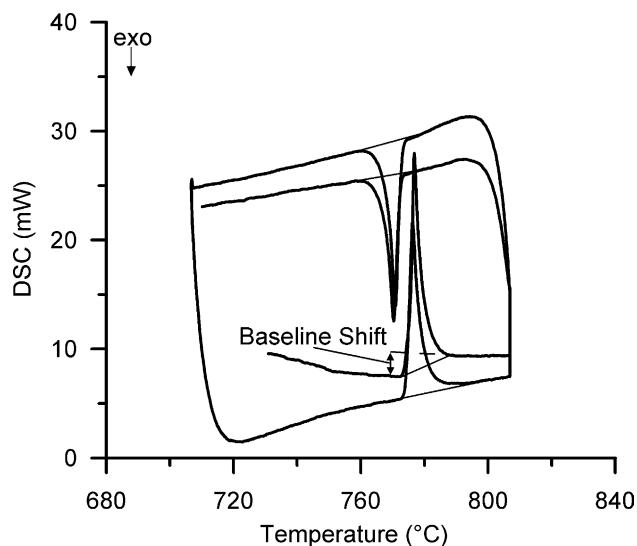


Fig. 12. DSC trace of Ag–Cu solid–liquid diffusion couple endotherm showing baseline shift on first cycle heating cycle only.

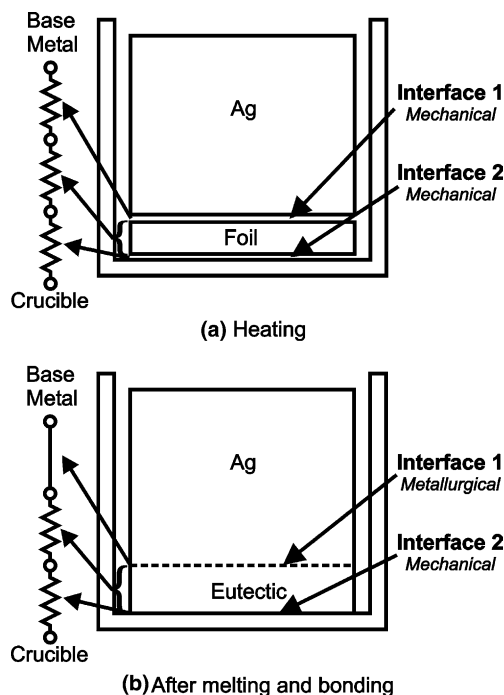


Fig. 13. Effects of melting on the thermal contact resistance in the DSC sample cell: (a) initial heating cycle and (b) subsequent heating cycles.

Since the nature of these interfaces change during initial heating they cause the observed baseline shift. However, once these interfaces develop a stable coupling as in Fig. 13(b), their influence is constant. This results in the much lower baseline shift observed in subsequent solidification and remelt peaks. This phenomenon is even more evident in the multi-thickness results of Table 3. The different foil masses were created by stacking the foils; which in turn, resulted in more interfaces between the diffusion couple stack-up and the crucible. As the number of interfaces increased, the baseline shift increased in magnitude see Table 4. Therefore, it can be concluded that the large baseline shift that is observed on the first heating segment is due to the effect of thermal coupling between the sample and the crucible; this induces error in the measurement of the melting endotherm and may contribute to the apparent fraction of liquid lost in the DSC results of Fig. 6.

Table 4  
Average baseline shift in DSC trace melting endotherm for diffusion couples with a stack of foils added to increase liquid width

Number of foils	Number of interfaces	Average $\Delta C$ (J)
1	2	10.8
2	3	22.2
3	4	24.3
4	5	37.9
5	6	35.5

#### 4.4. Correction methodology

An experimental procedure aimed at eliminating the thermal coupling artifact in the heating segment was designed. The sample was heated up to 800 °C, then immediately cooled through the freezing range before it was heated again to 800 °C. This preliminary cycle is used to remove the baseline shift effects from the initial heating segment and to establish a stable thermal interface. The short time of the first segment will have a minimal effect on the process kinetics. The results showed that the baseline shift during the initial melting segment increases the enthalpy measured from the DSC trace. The average ratio of initial to secondary melting enthalpies was 1.24.

An ensuing heating and cooling cycle was appended to the temperature program after the isothermal hold period. This provided an additional set of enthalpies with which to compare the solidification enthalpy after the isothermal hold period. The isothermal solidification kinetics can be determined using the additional data. There are now six enthalpies collected from each DSC diffusion couple experiment as shown in the sample temperature program of Fig. 14. The enthalpies M1 and S1 refer to the melting and solidification enthalpies, respectively, during the first heating and cooling cycle. Likewise, M2 and S2 refer to the melting enthalpy before and solidification enthalpy after the isothermal hold period. Finally M3 and S3 are the enthalpies of the final heating and cooling cycle.

The additional thermal peaks with the modified temperature program can be used to further analyze the process kinetics. Fig. 15 shows the results of the DSC diffusion couple experiments using the modified temperature program. The dataset S2/M1 is comparable to the original experimental results; however, the ratio S2/M2 eliminates the baseline shift effect, and shows only the ef-

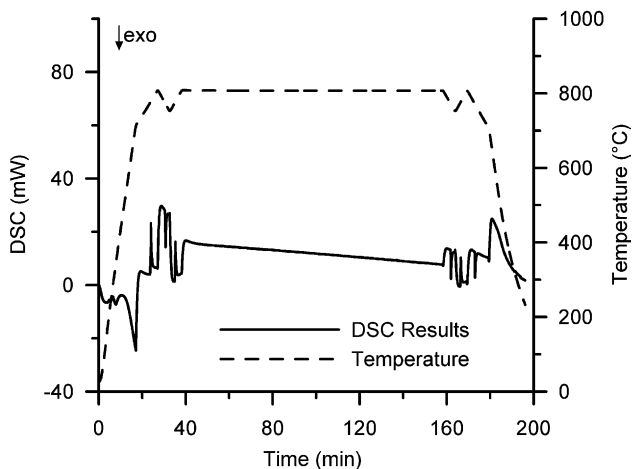


Fig. 14. Modified DSC temperature program with preliminary and ensuing heating cycles.

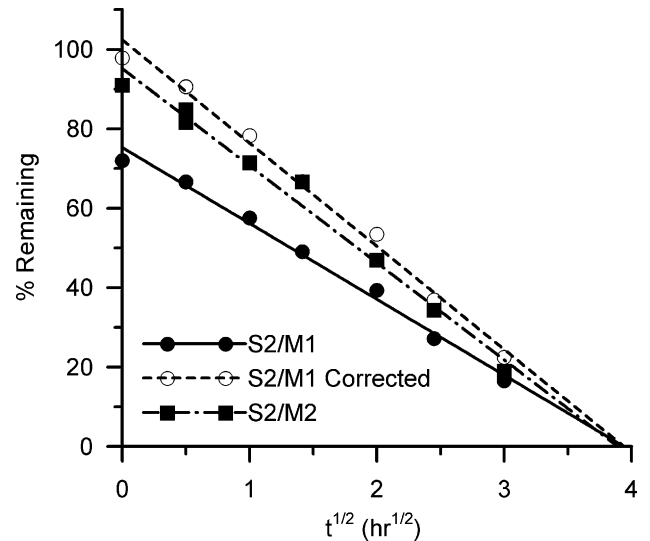


Fig. 15. DSC results using the modified temperature program.

fect of primary solidification (i.e., underestimate the fraction of liquid remaining). Furthermore, similar peaks can be compared, as shown in Fig. 16. The ratios S2/S1 and M3/M2 are the fractions of liquid remaining, taken from the solidification exotherms and melting endotherms, respectively, before and after the isothermal hold period. Fitted lines nearly pass through 100% at zero hold time as the experimental artifacts have been effectively removed from the measurement system.

The effects of primary solidification can be interpreted from the data by taking a ratio of solidification enthalpy to an adjacent melting enthalpy (e.g., S1/M2, S3/M3, or S2/M3). The average ratio values are about 0.91. From this data it can be deduced that the amount of liquid as measured by the solidification exotherm is about 9% less than that measured by the melting endo-

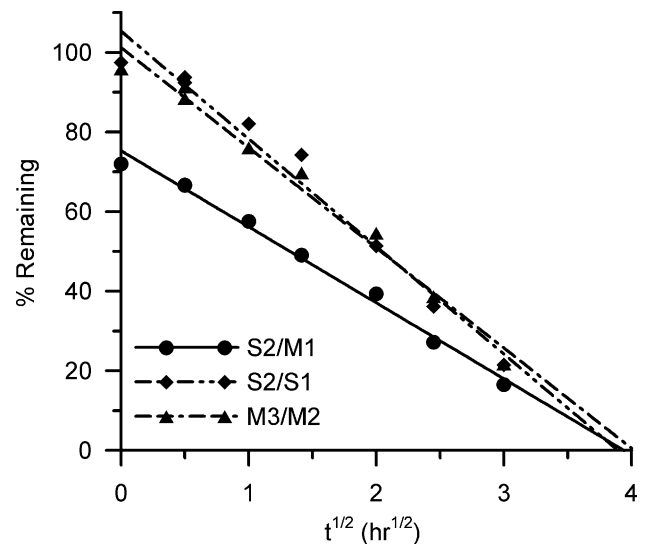


Fig. 16. Same as Fig. 15 except using ratios of similar peaks (e.g., S2/S1 or M3/M2).

therm for a given amount of liquid. This fraction is due to the combined effects of dissolution and primary solidification.

The original per cent liquid remaining data can be corrected for initial shift and primary solidification using the respective average ratios. Multiplication of the original enthalpy ratio as measured by the average initial shift (e.g., M1/M2, or 1.24) and the primary solidification (e.g., M3/S2, or 1.10) adjusts the data to account for the experimental artifacts. The correction factor is 1.36, and when applied to the original DSC results gives the per cent remaining shown in Fig. 17. The ratio S2/M1 is also corrected in Fig. 15. This corrected fraction of liquid remaining extrapolates back to unity at the vertical axis. The interface kinetics have now been accurately characterized and can be compared to other experimental setups such as different temperatures, foil thickness, or material systems.

The data collected from the DSC experiments can be comparatively examined using the time for isothermal solidification to be complete as predicted by extrapolation. An interface rate constant,  $\xi$ , describes the isothermal solidification kinetics and is independent of initial foil composition and maximum liquid width (Eq. (5)). This rate constant can be predicted using the analytical model given by Eq. (6). The variables needed for Eq. (6) are the partition coefficient,  $k$ , and the diffusivity,  $D$ . The liquidus composition at 800 °C as predicted by the equilibrium phase diagram is 24 wt.% (34.9 at.%), and the solidus composition is 7.8 wt.% (12.6 at.%) [12]. Thus, the partition coefficient (based on at.%) is 2.8. Selection of an appropriate value for the diffusivity of Cu in Ag is somewhat more difficult. Published values range from  $7.0 \times 10^{-10}$  cm<sup>2</sup>/s (for 6.6 at.% Cu) to  $4.9 \times 10^{-10}$  cm<sup>2</sup>/s (for 1.8 at.% Cu) [22]. The analytical model assumes a

constant diffusivity; however, the composition changes from 12.6% at the solid–liquid interface to 0% away from the interface. If the highest diffusivity is selected ( $7.0 \times 10^{-10}$  cm<sup>2</sup>/s), the predicted rate constant is  $-0.126$   $\mu\text{m}/\sqrt{\text{s}}$ , which compares exceptionally well with the measured values:

$$\xi = \frac{X(t)}{\sqrt{t}}, \quad (5)$$

$$\xi = -2(k-1)^{-1} \sqrt{\frac{D}{\pi}} \frac{\exp\left(\frac{-\xi^2}{4D}\right)}{\text{erfc}\left(\frac{\xi}{2\sqrt{D}}\right)}. \quad (6)$$

The time required for isothermal solidification as measured from the DSC diffusion couple experiments is 15.5 h, and the interface rate constant is  $-0.126$   $\mu\text{m}/\sqrt{\text{s}}$ , identical to that predicted by the analytical solution. The isothermal solidification time measured using the modified temperature program ranges from 15.2 to 16.2 h, depending on the method used. This corresponds to an interface rate constant in the range of  $-0.127$  to  $-0.123$   $\mu\text{m}/\sqrt{\text{s}}$ .

## 5. Conclusions

Interface kinetics in a binary (Ag–Cu) solid/liquid diffusion couple have been accurately quantified by comparing the endothermic melting peaks and exothermic solidification peaks on DSC traces generated from diffusion couples held at an elevated temperature for varying lengths of time. A novel methodology has been developed to characterize the mechanisms that induce error in the results. Experimental work has shown:

1. The presence of a relatively large mass of solid in the DSC crucible, acting as a heat sink, significantly affects the measured enthalpy, reducing the heat measured on both melting and solidification.
2. Epitaxial primary solidification of  $\alpha$ -phase during cooling from temperatures above the eutectic is not measured by the DSC resulting in a systematic underestimation of the liquid fraction remaining after an isothermal period.
3. A dramatic baseline shift across the first endothermic peak is a result of a change in the thermal contact resistance across the foil/base metal interface as the foil melts and wets the faying surface. Using a modified temperature program can eliminate this baseline shift, which induces error in the measurement of the initial melting endotherm.
4. Diffusion couple results from the modified temperature program experiments show that the effect of primary solidification is a 9% underestimation in the fraction of liquid remaining. Correction of the origi-

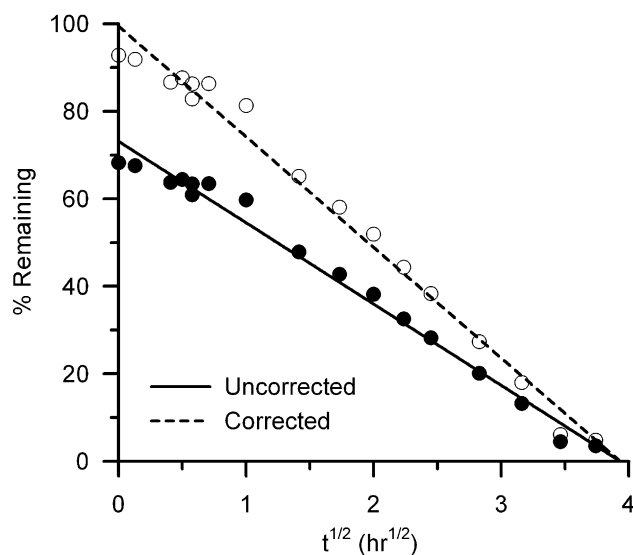


Fig. 17. DSC diffusion couple results corrected to extrapolate to unity at the abscissa.

nal data for primary solidification and the effect of baseline shift by a factor of 1.36 improves the agreement with modified temperature program results.

5. Interface kinetics predicted by the analytical model agree well with the experimental results. For the Ag–Cu system at 800 °C the predicted interface rate constant is  $-0.126 \mu\text{m}/\sqrt{\text{s}}$  whereas the measured values range from  $-0.127$  to  $-0.123 \mu\text{m}/\sqrt{\text{s}}$ .

### Acknowledgement

This research was supported by the Natural Sciences and Engineering Research Council of Canada.

### References

- [1] AWS Brazing and Soldering Committee. AWS brazing handbook. 4th ed. Miami (FL): American Welding Society; 1991. p. 5.
- [2] Purdy GR, Malakhov DV, Guha A. J Phase Equil 2001;22:439.
- [3] Tobiyama Y, Kato C. Tetsu-to-Hagane (J Iron Steel Inst Jpn) 2003;89:38.
- [4] Mortensen A, Jin I. Int Mater Rev 1992;37:101.
- [5] German RM, Dunlap JW. Metall Trans A 1986;17A:205.
- [6] Lumley RN, Shaffer GB. Scripta Mater 1996;35:589.
- [7] Maeda S. J Met Finish Soc Jpn 1986;37:430.
- [8] MacDonald WD, Eagar TW. Annu Rev Mater Sci 1992;22:23.
- [9] Corbin SF, Lucier P. Metall Mater Trans A 2001;32A:971.
- [10] Nakagawa H, Lee CH, North TH. Metall Trans A 1991;22A:543.
- [11] Sinclair CW. J Phase Equil 1999;20:361.
- [12] Subramanian PR, Perepezko JH. Ag–Cu binary alloy phase diagram. In: Baker H, editor. ASM handbook. Alloy phase diagrams, vol. 3. Materials Park (OH): ASM International; 1992. p. 228.
- [13] Zhou Y, Gale WF, North TH. Int Mater Rev 1995;40:181.
- [14] Brown ME. In: Introduction to thermal analysis. New York (NY): Chapman and Hall; 1988. p. 29.
- [15] Zhou Y, Kuntz ML, Corbin SF. In: Joining of advanced and specialty materials V, materials solutions '02. Materials Park (OH): ASM International; 2003. p. 75.
- [16] Saida K, Zhou Y, North TH. J Japan Inst Metals 1994;58:810.
- [17] Campbell CE, Boettinger WJ. Metall Trans A 2000;31A:2835.
- [18] Porter DA, Easterling KE. In: Phase transformations in metals and alloys. 2nd ed. London: Chapman and Hall; 1992. p. 322–6.
- [19] Hamana D, Boumerzoug Z. Mater Sci Forum 1999;294–296:593.
- [20] Venkatraman R, Wilcox JR, Cain SR. Metall Mater Trans A 1997;28A:699.
- [21] Cain SR, Wilcox JR, Venkatraman R. Acta Mater 1997;45:701.
- [22] Cahoon JR, Youdelis WV. In: Smithells metals reference book. 6th ed. London: Butterworths; 1983. p. 13–55.